

## DESIGN OF THE PROPOSED 250 MEV SUPERCONDUCTING CYCLOTRON MAGNET

M. K. Dey<sup>#</sup>, A. Dutta Gupta, U. Bhunia, S. Saha, A. Dutta, J. Pradhan, S. Sur, S. Murali, J. Chaudhuri, C. Mallik and R.K. Bhandari  
Variable Energy Cyclotron Centre, Kolkata

### Abstract

VECC has proposed a project for the design and development of a 250 MeV superconducting proton cyclotron, which may be used in therapy. In this paper we describe the preliminary design calculations for the superconducting cyclotron magnet. Hard-edge approximation method has been adopted for finding the poletip geometry to meet the basic focusing requirements of the beam. The uniform-magnetization method has been applied to calculate the 3D magnetic field distribution due to saturated iron poletips, to verify the beam dynamical issues and optimize the poletip geometry. GM type closed cycle cryo-cooler technology is being considered for steady state liquefaction of evaporated helium gas from magnet cryostat.

### INTRODUCTION

Basic design parameters are decided by the requirements for medical application of the cyclotron, i.e., for the treatment of deep seated cancerous tumors. Proton energy of 250 MeV corresponds to approximately 40 cm penetration range in water. The cyclotron is targeted to be designed for delivering a few hundreds of nano-amperes beam current.

The design of the cyclotron magnet is an iterative process. Approximate hard-edge formulas are used to determine the basic dimensions and geometry of the poletip sectors [1, 2]. The 3D software TOSCA has been used to calculate median plane magnetic field distribution (fig 1). Since the superconducting magnet is operated in high field level (peak hill field at median plane  $\sim 3.6\text{T}$ ), the pole-tip iron is fully saturated. So the uniform-magnetization method is adopted to simulate the azimuthal variation of the field due to spiral hill-valley structure of the magnet [3]. This makes the iterative optimization of the poletip geometry faster. Orbit tracking codes are used to calculate the equilibrium orbit properties.

The cryogenic system primarily consists of helium reservoir, GM type cryo-cooler, magnet cryostat with multilayer insulation and 80 K radiation shield inside, conduction cooled current leads, etc. The cold mass can be slowly cooled down from room temperature to reach liquid helium temperature either by directly coupling the cryostat with helium refrigerator or initially by liquid nitrogen and then by liquid helium. The evaporated helium gas from the cryostat will be reliquefied by condensing it through the cold head of the multistage GM type cryo-cooler. This is a very new and economic technology compared with the conventional technique of

<sup>#</sup>malay@veccal.ernet.in

coupling with liquid helium plant (as used in VECC K500 superconducting cyclotron magnet).

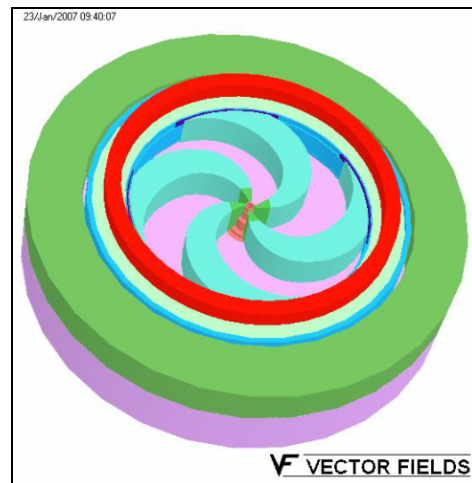


Figure 1: TOSCA model of upper half of cyclotron magnet.

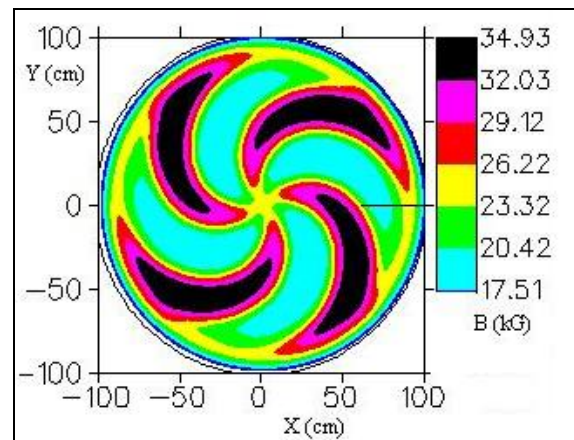


Figure 2: Contour plot of median plane magnetic field.

### SECTOR GEOMETRY

To minimize the size and cost of the cyclotron it is desirable to operate at maximum possible magnetic field strength. But with stronger magnetic field, higher electric field is required at the deflector system to extract the beam, so making the extraction process very difficult and unstable. Moreover, since the fractional azimuthal variation of the field (flutter) decreases with increasing average field, stronger spiralling of the sector is required to compensate for the decrease in vertical focusing, causing manufacturing challenge. So an optimum value of

~2.37T is chosen for the central field  $B_o$ , for which the orbital rotational frequency is ~36.14 MHz. A four-sector cyclotron magnet is more suitable for 250 MeV proton beam than a three sector magnet like VECC K500 cyclotron, to avoid the proximity of  $\nu_r = 3/2$  stop-band [4].

The average isochronous field is given by  $B_{av} = B_o \gamma$ , where,  $\gamma = 1+T/E_o$ ,  $T$  is the kinetic energy and  $E_o$  is the rest mass energy. The average radius of the equilibrium orbit is given by  $R = (T^2 + 2 T E_o)^{0.5} / (300 \gamma B_o q)$ , where  $q$  is charge of the particle. Once the hill and valley fields ( $B_h, B_v$ ) are decided, the required isochronous field determines the sector angles. The angular width of the sector angles are given by

$$\eta_h = \frac{2\pi}{N} \cdot \frac{(B_{av} - B_v)}{(B_h - B_v)} \quad \eta_v = \frac{2\pi}{N} - \eta_h$$

Then spiral angle is introduced to the hill-valley sectors to enhance the vertical focussing. In the initial design stage we rely on first order beam optics using hard-edge model. The transfer matrix for the cyclotron magnet can be composed, assuming it as a series of sector magnets with constant fields ( $B_h$  or  $B_v$ ) and the edge matrices defined by spiral angles. Focusing frequencies are given by,

$\nu_r = (N/2\pi) \cdot \cos^{-1}(Tr(M_r)/2)$ ,  $\nu_z = (N/2\pi) \cdot \cos^{-1}(Tr(M_z)/2)$ , where  $Tr$  stands for trace of the matrix,  $M_r$  and  $M_z$  are transfer matrices for one sector of the cyclotron in radial and vertical planes respectively.

With the sector geometry, found by hard-edge model, magnetic field in the median plane of the cyclotron is calculated with TOSCA and uniform magnetization method (fig 2). Equilibrium orbit behaviour is investigated by orbit tracking (fig 3). At this stage, several iterations were required to optimise the sector geometry.

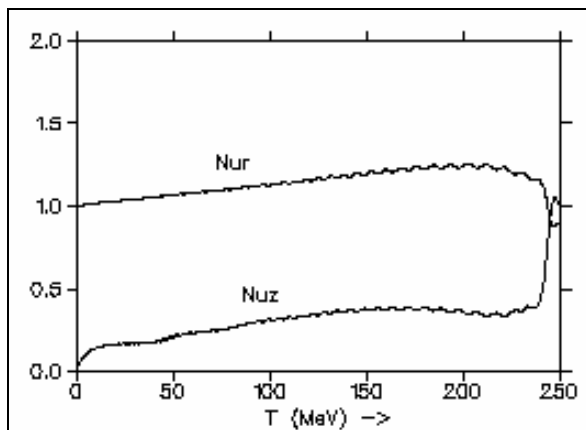


Figure 3: Radial and vertical tunes vs. kinetic energy.

### COIL AND CRYOSTAT GEOMETRY

Cryostat for the proposed 250 MeV cyclotron has a stainless steel annular bobbin on which superconducting

coil (Nb-Ti) will be wound at a pre-tension of about 80 MPa. The preliminary design of the cryostat looks like the one shown in figure 4.

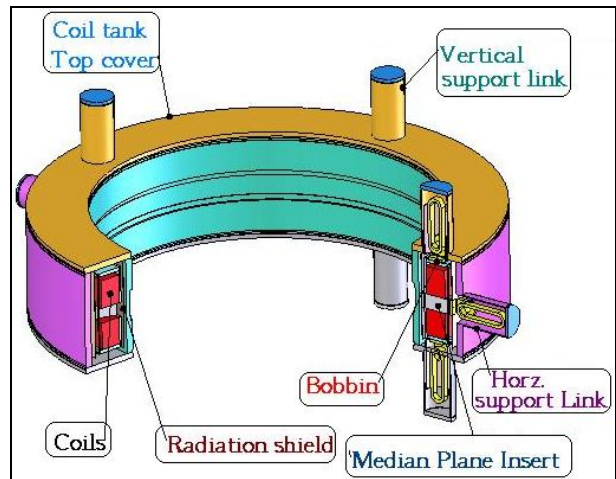


Figure 4: Preliminary design sketch of the cryostat.

Temperature distribution after cool down of magnet cryostat to liquid helium temperature is as shown in fig 5.

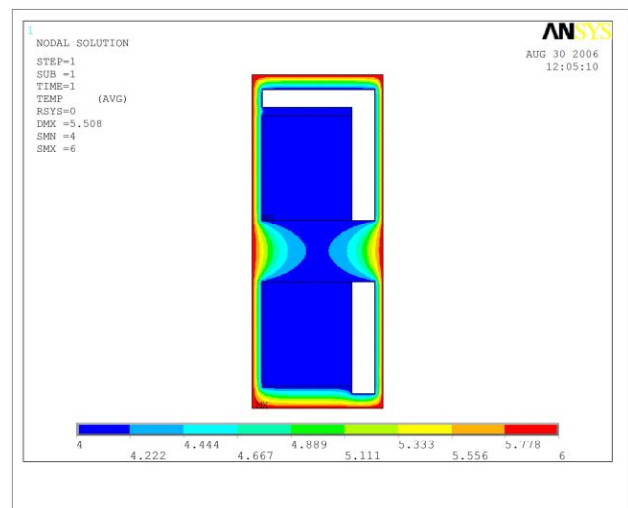


Figure 5: Temperature distribution in the coil & bobbin.

Figure 6 shows the magnetic field distribution in place of coil and cryostat. A preliminary one dimensional calculation was made and the radial and tangential stress distribution is plotted in the figure 7 and figure 8 [5].

The bobbin is made of stainless steel. It is estimated the heat load to the LHe could be kept below 6 watts. Hence, the cryocooler based cooling system may be considered instead of conventional LHe plant system. Both of direct conduction cooling or recondensing bath cooling may be considered before deciding over the methodology of operation. The second stage of the cryocooler is used to cool the copper radiation shields.

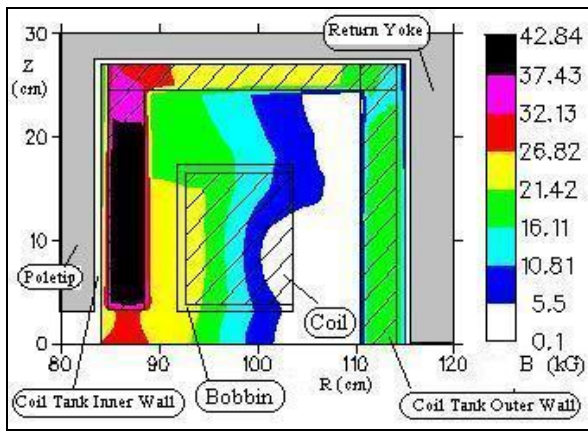


Figure 6: Magnetic field distribution in place of coil.

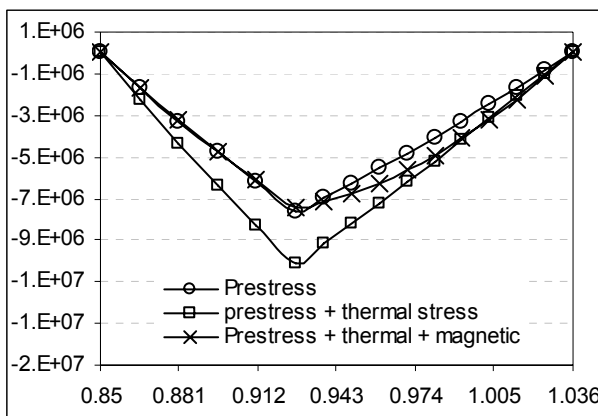


Figure 7: Radial stress distribution

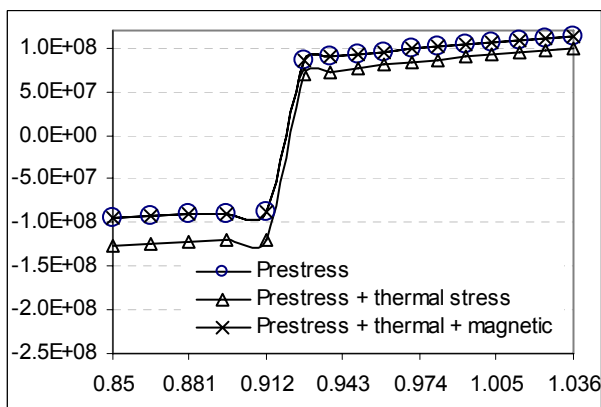


Figure 8: Tangential stress distribution

The 8 vertical and 4 horizontal support links of equal lengths support the liquid helium mass inside the vacuum chamber. The vacuum chamber is made of iron to reduce the return path iron requirements.

There is cooled radiation shield around the median plane penetrations to reduce the direct heat load to LHe from room temperature. All the supports and access pipes

have intermediate temperature intercepts to reduce the conduction heat load.

### CONCLUSION

The preliminary design study suggests the feasibility of developing such a cyclotron for therapeutic use. Detail design calculation is under progress. Primary design of superconducting magnet coil, cryostat, etc. has been completed. Cryo-condensation system of saturated helium gas at 4.5 K has to be practically demonstrated using multistage GM type cryo-cooler.

### REFERENCES

- [1] J.J.Livingood, Cyclic Particle Accelerator (Princeton, 1961). p. 42.
- [2] K.G. Stephen, High Energy Beam Optics (New York, 1965), P. 100.
- [3] M.M. Gordon and D.A. Johnson, Particle Accelerator, 1980, Vol.10, p.217-222.
- [4] J. Kim and H. Blosser, International Conference on Cyclotrons and Their Applications, 2001, p.345.
- [5] Martin N. Wilson, Superconducting Magnets, Clarendon Press Oxford, 1983, p 41.